AD NUMBER

AD-855 156

CLASSIFICATION CHANGES

TO **UNCLASSIFIED**

FROM **NEVER CLASSIFIED**

AUTHORITY

U.S. Army Materiel Command, Washington, DC; June 1969.

19990301070

THIS PAGE IS UNCLASSIFIED

AD NUMBER

AD-855 156

NEW LIMITATION CHANGE

TO

DISTRIBUTION STATEMENT - A

Approved for Public Release; Distribution Unlimited.

LIMITATION CODE - 1

FROM

DISTRIBUTION STATEMENT - NONE

No Prior DoD Distribution Security Control Statement.

AUTHORITY

Army Ballistic Research Lab., via ltr. dtd April 22, 1981.

BRL

AD

MEMORANDUM REPORT NO. 1983

AN EXPERIMENTAL INVESTIGATION AT SUPERSONIC MACH

NUMBERS OF BASE DRAG OF VARIOUS BOATTAIL SHAPES

WITH SIMULATED BASE ROCKET EXHAUST

by

Joseph Huerta

JUL 23 1969

June 1969

U.S. ARMY ABERDEEN RESEARCH AND DEVELOPMENT CENTER
BALLISTIC RESEARCH LABORATORIES
ABERDEEN PROVING GROUND, MARYLAND

43

BALLISTIC RESEARCH LABORATORIES

MEMORANDUM REPORT NO. 1983

JUNE 1969

AN EXPERIMENTAL INVESTIGATION AT SUPERSONIC MACH NUMBERS
OF BASE DRAG OF VARIOUS BOATTAIL SHAPES
WITH SIMULATED BASE ROCKET EXHAUST

Joseph Huerta

Exterior Ballistics Laboratory

RDT&E Project No. 1T061102A33D

ABERDEEN PROVING GROUND, MARYLAND

BALLISTIC RESEARCH LABORATORIES

MEMORANDUM REPORT NO. 1983

JHuerta/lca
Aberdeen Proving Ground, Md.
June 1969

AN EXPERIMENTAL INVESTIGATION AT SUPERSONIC MACH NUMBERS
OF BASE DRAG OF VARIOUS BOATTAIL SHAPES
WITH SIMULATED BASE ROCKET EXHAUST

ABSTRACT

An experimental investigation was conducted to determine the effect
of boattail geometry and simulated base rocket nozzle flow on overall
base drag. All tests were performed at Mach numbers 2.50, 3.00 and
3.50. Reasonable prediction of base drag for the reported boattail
shapes can be made by using approximate and empirical equations. A
conical boattail produced less drag than the other boattail shapes
investigated. The maximum nozzle stagnation to free-stream pressure
ratio reported is 315.

TABLE OF CONTENTS

LIST OF ILLUSTRATIONS

LIST OF SYMBOLS

a_j^* sonic velocity at jet exit conditions

m_i mass flow based on A_B and free stream conditions

m_j mass flow through sustainer nozzle

p_b average base pressure

p_c sustainer nozzle stagnation pressure

p_j jet exit static pressure

p_ℓ local static pressure

p_∞ free-stream static pressure

p_2 static pressure downstream of a corner

q free-stream dynamic pressure

r radius of body at point x

s rectangular coordinate in streamline direction

x coordinate measured from vertex of body

x_2 position of a corner

A_B maximum body area

A_b base area

A_j jet exit area

A_ℓ increment of area associated with the local static pressure

C_{DB} base drag coefficient

C_{DBT} boattail drag coefficient

C_1 characteristic coordinate along Mach line

D_b base diameter

D_j jet exit diameter

M Mach number

9

LIST OF SYMBOLS (Continued)

M_j jet exit Mach number

M_j^* dimensionless jet velocity, V_j/a_j^*

M_∞ free-stream Mach number

P_o tunnel stagnation pressure

Re   free-stream Reynolds number

V_j jet exit velocity

V_ℓ local velocity

γ ratio of specific heats

δ flow deflection angle

δ_1 flow deflection angle before a corner

δ_2 flow deflection angle after a corner

μ Mach angle (arcsin 1/M)

I. INTRODUCTION

Methods for reducing missile drag, especially base drag, have been of considerable practical importance. As a consequence, the Army Missile Command (MICOM), Redstone Arsenal, Alabama, has been conducting a continual program to investigate techniques for minimizing missile base drag. As a part of this continuing investigation, the present tests were conducted in the supersonic wind tunnel of the Ballistic Research Laboratories (BRL) to determine the effect of six boattail configurations on drag. Base drag was measured in the presence of a sustainer rocket motor exhausting cold flow through the base. A comparison of experimental data and a second-order shock-expansion method for boattail-pressure distribution was made. An empirical technique was employed to estimate "power on" base drag and these results are compared with measured data.

The basic model was a strut-mounted body of revolution. The section forward of the boattail consisted of a tangent-ogive nose followed by a cylindrical center body. Pressure data were obtained along the boattail surface and model base at nominal test Mach numbers of 2.50, 3.00 and 3.50 for each boattail shape with the model at zero angle of attack. Sustainer nozzle pressure was also varied for each boattail. The ratio of nozzle exit diameter to body diameter was 0.200 and the nozzle exit Mach number was 2.7 for fully developed flow or "power on" condition.

II. APPARATUS

A. Wind Tunnel

Supersonic Wind Tunnel No. 1 of the Ballistic Research Laboratories was used to acquire the data. This is a two-dimensional continuously operated, variable density, closed circuit tunnel having a test section 15 inches high and 13 inches wide. Two flexible steel plates form the upper and lower walls of the nozzle section. A complete description of this facility and its flow characteristics are given in References 1 and 2.

11

B. Test Model

The model was a body of revolution attached to the upper test
section wall by a swept back support strut at zero angle of attack. It
consisted of a tangent-ogive nose attached to a cylindrical center body
and ending with a boattail. Figure 1 shows a photograph of the model
installation in the test section and the schematic of Figure 2 presents
the pertinent dimensions of the model and support strut. The overall
length of the model was 15.0 inches and the diameter was 2.500 inches.
The support strut was a modified double wedge section, 0.435 inch thick
with a 3.125 inches chord. The exit diameter of the sustainer nozzle
was 0.500 inch or 0.200 calibers and the exit Mach number was 2.7.
Model pressure taps were placed opposite the model support strut and
located on the cylindrical surface, boattail surface and at the base.
The photograph of Figure 3 presents a view of these pressure taps.

Six boattail configurations were investigated in this program.
All of these boattails were one caliber in length. Figures 4 and 5
define the geometric shapes of these boattails which consisted of conical,
concave, convex and reverse curvature configurations.

C. Instrumentation

The model pressures were transmitted through metal tubing to a
pressure scanner system. The pressure scanner (Figure 6) is a solid
metal block which is channeled such that, with the aid of pneumatically
operated valves, seals and stepping switches, pressures can be measured
in sets of seven pressures per cycle. This scanner unit is necessary
since the tunnel automatic data acquisition system is capable of handling
only eight inputs per sampling time. Pressures from the scanner were
measured by a group of pressure transducers of suitable pressure range.
The electrical output signals from these transducers were converted by
an automatic readout system to digital readings which were recorded
automatically by typewriter. A complete description of the scanner is
given in Reference 3.

The sustainer nozzle total pressure and tunnel total pressure were monitored continuously throughout the period of data acquisition. The sustainer nozzle stagnation pressure was measured in its plenum chamber.

A schlieren system with camera provides continuous visual indication, as well as photographs, of the flow conditions in the test section.

III. TEST PROCEDURE AND CONDITIONS

The flow in the wind tunnel was established at a low stagnation pressure and then the pressure was raised to the desired level. The sustainer nozzle pressure was adjusted to the proper value. With all flow conditions at steady state, model pressure readings were obtained with the pressure scanner system. Before each set of model pressures were recorded, it was ascertained that these pressures were stabilized in the scanner system by observing their respective dial readings on the control panel. Pressure readings were recorded when all dial motion ceased. After making a complete pressure sampling cycle, the jet pressure was adjusted to the next value, and the model pressure reading cycle was repeated. The available line pressure for the sustainer nozzle was 300 psia. The variation in tunnel stagnation and sustainer nozzle pressure was less than 0.1 percent.

The average tunnel operating conditions are listed in Table I for the three Mach numbers. The specific humidity was maintained below 0.0002 pound of water per pound of air. Schlieren photographs were taken of the flow field for selected model configurations.

Table I. Tunnel Operation Conditions

Mach No.	P_o psia	q psi	Re x 10^{-6} per inch
2.50	28.88	7.40	0.50
3.00	40.45	6.94	0.50
3.50	52.69	5.92	0.50

A narrow band of fine grit was placed on the nose surface near the tip to insure a turbulent boundary layer at all times.

IV. DATA REDUCTION

The raw pressure data were converted into the required ratio and coefficient form by a computer. The data acquisition system automatically recorded the raw data from the pressure transducers in digital typewritten and coded punched tape form. The punched tape was used to obtain punched cards which were fed into the computer for reduction and tabulation of the raw data into the desired form.

The local pressures were weighted by area to determine the boattail and base drag coefficients. The boattail and base drag coefficients were calculated from the following general relationship

$$C_D = \frac{-\sum_{i=1}^{n} [(p_{\ell_i} - p_\infty) A_i]}{q A_B} \qquad \begin{array}{l} n = \text{number of} \\ \quad \text{local pressures} \\ \quad \text{and associated} \\ \quad \text{incremental areas} \end{array}$$

where p_ℓ is the local pressure. The area, A, used to calculate boattail drag is the local area, A_ℓ, projected on the vertical plane. The overall error in determining the model static pressures was approximately $\pm .003$ psi.

V. DISCUSSION OF THEORETICAL AND EMPIRICAL CALCULATIONS

The equation for the streamwise pressure gradient is given as

$$\frac{\partial p}{\partial s} - \frac{2 \gamma p}{\sin 2\mu} \frac{\partial \delta}{\partial s} = \frac{1}{\cos \mu} \frac{\partial p}{\partial C_1}$$

In obtaining the Prandtl-Meyer relation, the pressure is considered constant along the first-family Mach lines. Therefore, the right hand part of the above equation becomes zero and the solution of the integrated equation is the Prandtl-Meyer relation. The second-order shock expansion method imposes a different condition on the pressure gradient equation to obtain an approximate solution (Reference 5).

14

First consider a body of revolution with a pointed nose and supersonic flow on its surface. Drawing a series of tangent lines to this body contour results in an approximate shape consisting of a series of frustums with a cone vertex. Now on this new geometric shape, it can be assumed that the flow direction does not change within a single element. Now it can be stated that $\partial \delta/\partial s = 0$ and the pressure gradient equation reduces to

$$\frac{\partial p}{\partial s} = \frac{1}{\cos \mu} \frac{\partial p}{\partial C_1}$$

The solution to the above differential equation is the second-order shock expansion method which is

$$p = p_f - (p_f - p_2) \; e^{-\eta}$$

where p_f = pressure on a cone tangent to the body at the same point as a frustum element

$$\eta = \left(\frac{\partial p}{\partial s}\right)_2 \frac{x - x_2}{(p_f - p_2) \cos \delta_2}$$

$$\left(\frac{\partial p}{\partial s}\right)_2 = \frac{B_2}{r} \left(\frac{\Omega_1}{\Omega_2} \sin \delta_1 - \sin \delta_2\right) + \frac{B_2}{B_1} \frac{\Omega_1}{\Omega_2} \left(\frac{\partial p}{\partial s}\right)_1$$

$$B = \frac{\gamma \, p \, M^2}{2 \, (M^2 - 1)} = \frac{q}{M^2 - 1}$$

and

$$\Omega = \frac{1}{M} \left[\frac{1 + \left(\frac{\gamma - 1}{2}\right) M^2}{\frac{\gamma + 1}{2}}\right]^{\frac{\gamma + 1}{2 (\gamma - 1)}}$$

The above equation for Ω is the one dimensional area ratio. Now the second-order equation gives the pressure variation along the surface of the body.

Only the boattail surface pressures are of interest here, so the foregoing second-order equation is further simplified by imposing the following conditions:

1. $(\partial p/\partial s)_1 = 0$

2. $p_f = p_\infty$ or $p_1 = p_\infty$

3. $x = 0$ at the start of the boattail which eliminates the dimension x_2

The following sketch shows that $\delta_1 = 0^\circ$, and δ_2 is a negative angle.
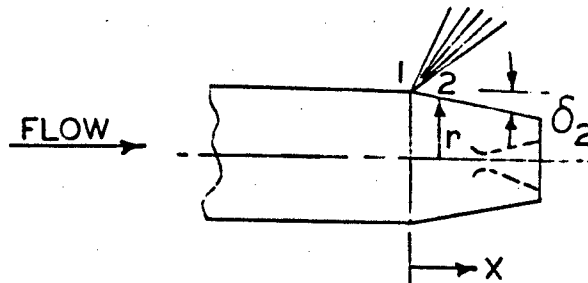
The boattail pressure distributions were calculated from the following set of simplified equations.

$$p = p_\infty - (p_\infty - p_2)\, e^{-\eta}$$

$$\eta = \left(\frac{\partial p}{\partial s}\right)_2 \frac{}{(p_\infty - p_2)\cos \delta_2}$$

$$\left(\frac{\partial p}{\partial s}\right)_2 = -\frac{B_2}{r}\sin \delta_2$$

$$B_2 = \frac{\gamma\, p_2\, M_2^2}{2\,(M_2^2 - 1)}$$

The presence of nozzle flow at the base adds to the complexity of the flow mechanism at the base which is difficult to analyze. Consequently, empirical results have been sought by correlation of available experimental data (Reference 6). A reasonable base pressure prediction

16

for a base with nozzle flow can be made by use of the following empirical equation:

$$\frac{p_b}{p_\infty} = \frac{1}{M_j^*} \left[\frac{3.5}{1 + 2.5 \, (A_b/A_B)}\right] \left[0.19 + 1.28 \left(\frac{R_{mf}}{1 + R_{mf}}\right)\right]$$

where

$$R_{mf} = \frac{(\dot{m} \, V)_j}{(\dot{m} \, V)_\infty} = \frac{\gamma_j \, p_j \, A_j \, M_j^2}{\gamma_\infty \, p_\infty \, A_B \, M_\infty^2}$$

The base drag coefficient is then calculated by use of the equation:

$$C_{D_B} = \frac{2}{\gamma_\infty \, M_\infty^2} \left(1 - \frac{p_b}{p_\infty}\right) \left(\frac{A_b - A_j}{A_B}\right)$$

VI. PRESENTATION AND DISCUSSION OF DATA

Figures 7 through 9 present data of the boattail portion of all test configurations. The curves in Figures 10, 11 and 12 indicate results of base measurements for these configurations. A comparison of total drag (boattail and base drag) for configurations 6, 7 and 8 is presented in Figure 13. The test data presented are for test Mach numbers of 2.50, 3.00 and 3.50.

The boattail surface pressure distributions were determined for the six boattail configurations and typical distributions are presented in Figure 7 as a function of distance in calibers from the boattail corner. For boattail configurations 6, 7 and 8, there are included, for comparison, pressure distribution curves obtained by the method of characteristics at Mach numbers 2.50 and 3.00 and by the second-order shock expansion method of Reference 5 for all three Mach numbers. Configuration 11 data are presented for Mach numbers 2.50 and 3.00 with the method of characteristic curves included for comparison. Either method appears to predict the pressure distribution of these boattails well for

17

at least the last two-thirds of the boattail surface. The wide differences between experimental points and the curves at the beginning of the boattail must be due to the boundary layer present at the corner.

The data of Figure 8 provides evidence that the flow from the sustainer nozzle has negligible effect on the boattail drag. The boattail drag coefficient of each boattail configuration appears unchanged for all base flow conditions.

The variation in boattail drag with Mach number is shown in Figure 9. It appears that the conical boattail configuration 6 offers the least drag when compared to other boattail shapes having the same base diameter.

The data of Figure 10 indicate the influence of the base nozzle flow on base pressure for the case of fully developed flow in the nozzle. Results for configurations 6, 7 and 8 are presented. The results of configuration 6 apply to configurations 9, 10 and 11 as well. The method of Reference 6 for predicting base pressure was utilized in calculating the curves shown with these data for comparison. Reasonable predictions of base pressure can be made with this empirical method. However, it appears that the ratio of nozzle diameter to base diameter has a strong influence on accuracy of the prediction. The results in Figure 11 are the base pressure data of Figure 10 reduced to base drag coefficient form and the comments made on Figure 10 data apply to these also. The base drag as a function of the sustainer jet flow parameter is displayed in Figure 12. These curves show that the base drag for configurations 6, 9, 10 and 11 is the same as was pointed out above.

A comparison of total drag (boattail and base drag) for the three conical boattails and a square base configuration from Reference 7 is shown in Figure 13. Only slight differences in total drag are indicated for the conical boattails. However, the square base configuration has about 60 percent more drag than the conical boattail configurations.

18

The schlieren photographs of Figure 14 show the flow field at the base for configuration 6 at Mach numbers 2.50 and 3.50 for base jet flow off and on.

VII. CONCLUSIONS

From this investigation, it can be concluded that less total drag results from a conical boattail configuration than any of the other contours tested.

Boattail pressure distribution can be determined over at least the last two-thirds of a conical boattail surface using the approximate shock-expansion method of Reference 5 which is much easier to use than the method of characteristics.

A reasonable prediction of base drag with rocket flow at the base can be made using the empirical method of Reference 6.

AMICOM BASE DRAG
BOATTAIL NO 6
MODEL M931
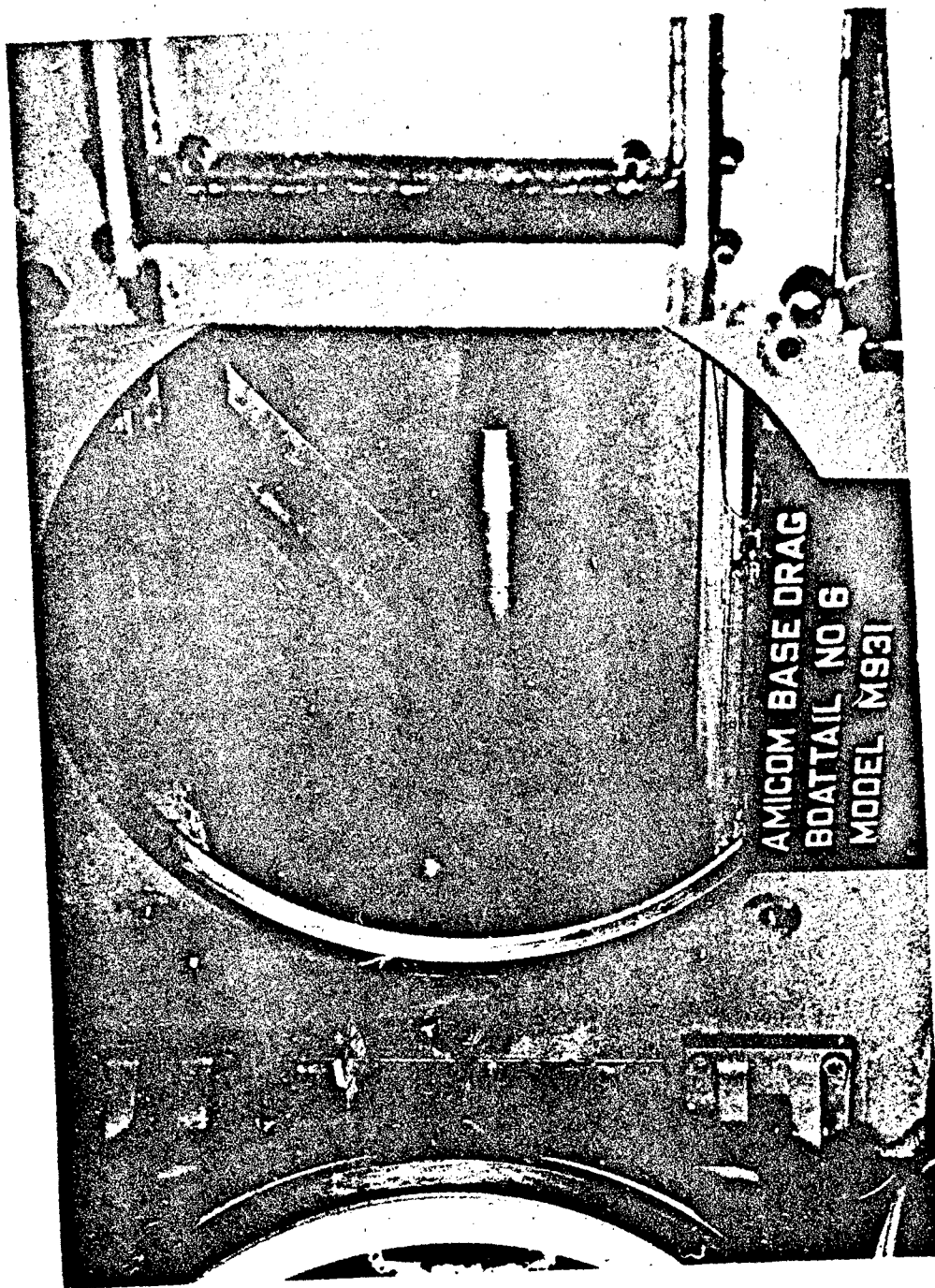
Figure 1. Typical Model Installation in the Wind Tunnel

MODEL SURFACE TAP LOCATION	
TAP	DISTANCE FROM BASE
1	3.366
2	2.964
3	2.564
4	2.434
5	2.138
6	1.842
7	1.546
8	1.250
9	0.954
10	0.658
11	0.362
12	0.066
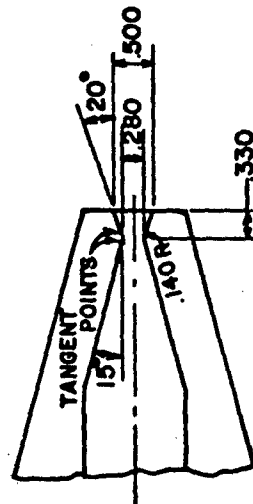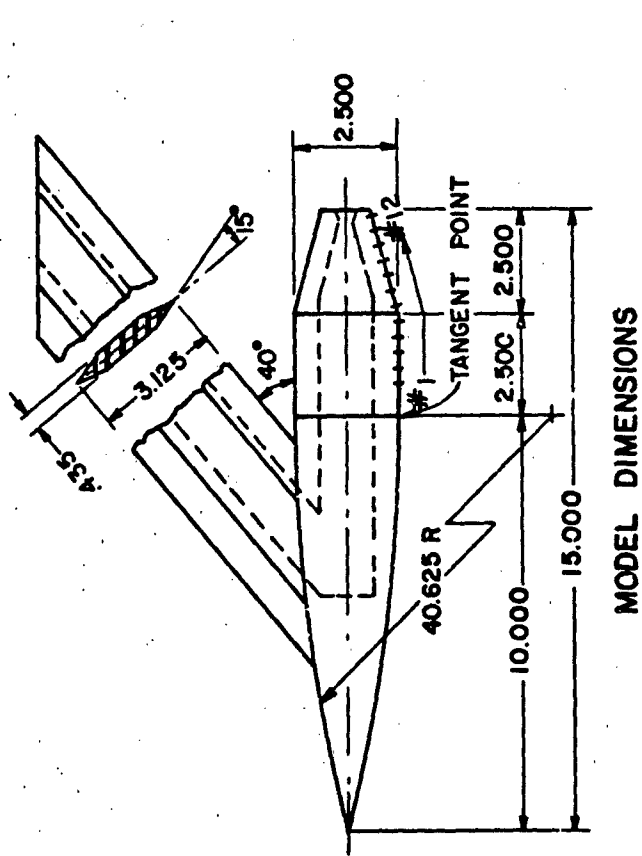
MODEL DIMENSIONS

NOZZLE DIMENSIONS

Figure 2. Model Dimensions and Boattail Tap Locations

Figure 3. Close Up of Model Pressure Taps
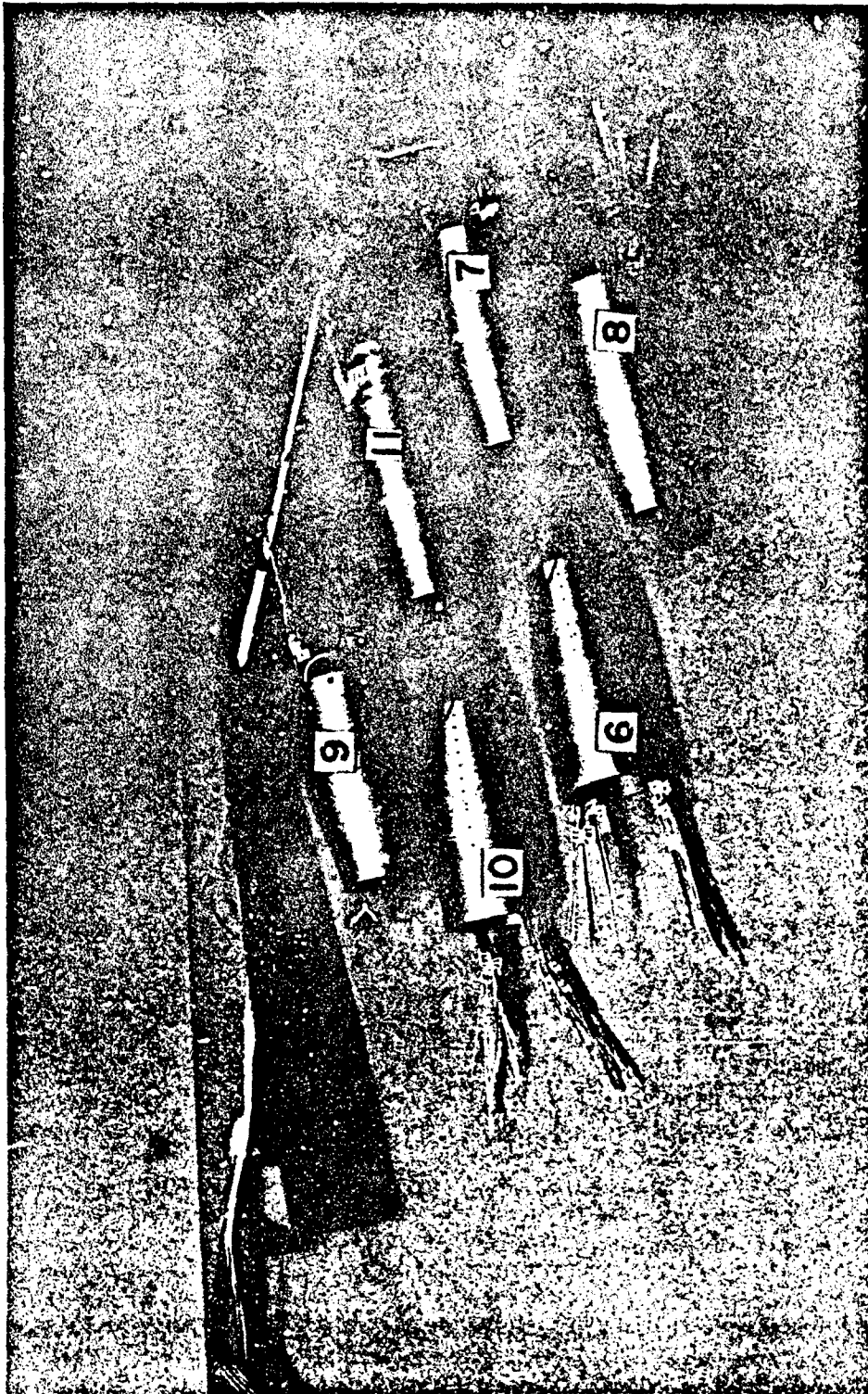
Figure 4. Boattail Configurations
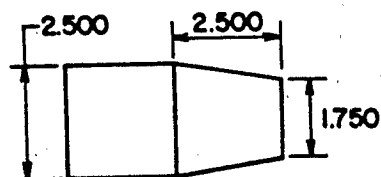
BOATTAIL NO.6
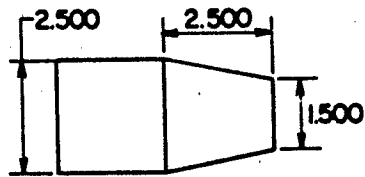
2.500 — 2.500 — 1.750

BOATTAIL NO.7

2.500 — 2.500 — 1.500

BOATTAIL NO. 8

2.500 — 2.500 — 1.250

BOATTAIL NO.9

$$\frac{r}{d} = 0.5\left[1.0 - 0.9\left(\frac{y}{d}\right)^2 + 0.6\left(\frac{y}{d}\right)^3\right]$$

2.500 — y — 1.750 — 2.500

BOATTAIL NO.10

2.500 — 2.500 — 1.750 — 8.521R

BOATTAIL NO.11

2.500 — 2.500 — 1.750 — 8.521R

.430 .561 .667 .759 .825
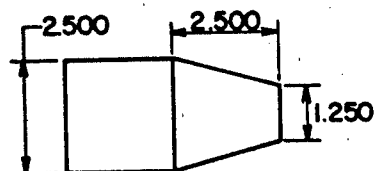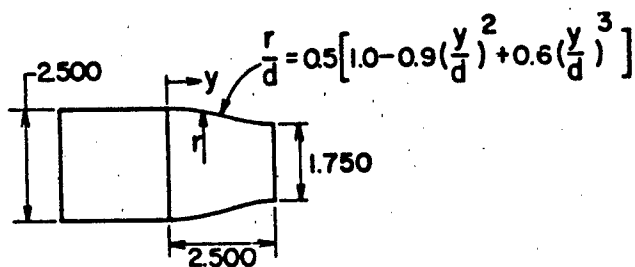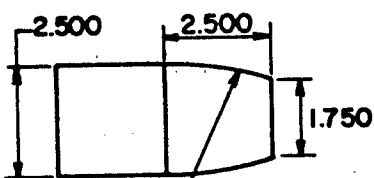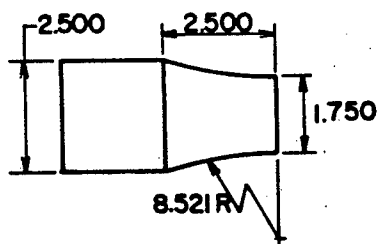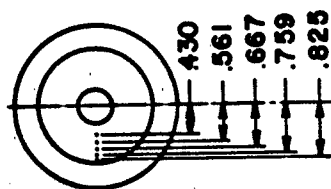
TAP LOCATION
ON BASE
CONFIG. 6,9,10,11

.430 .542 .634 .700
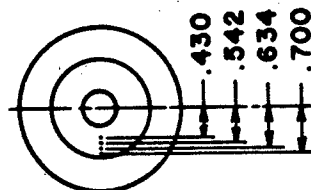
TAP LOCATION
ON BASE
CONFIG. 7

.430 .516 .575
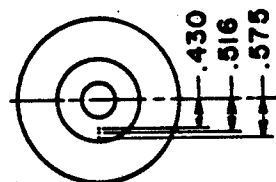
TAP LOCATION
ON BASE
CONFIG. 8

Figure 5. Boattail Dimensions and Base Tap Locations

24
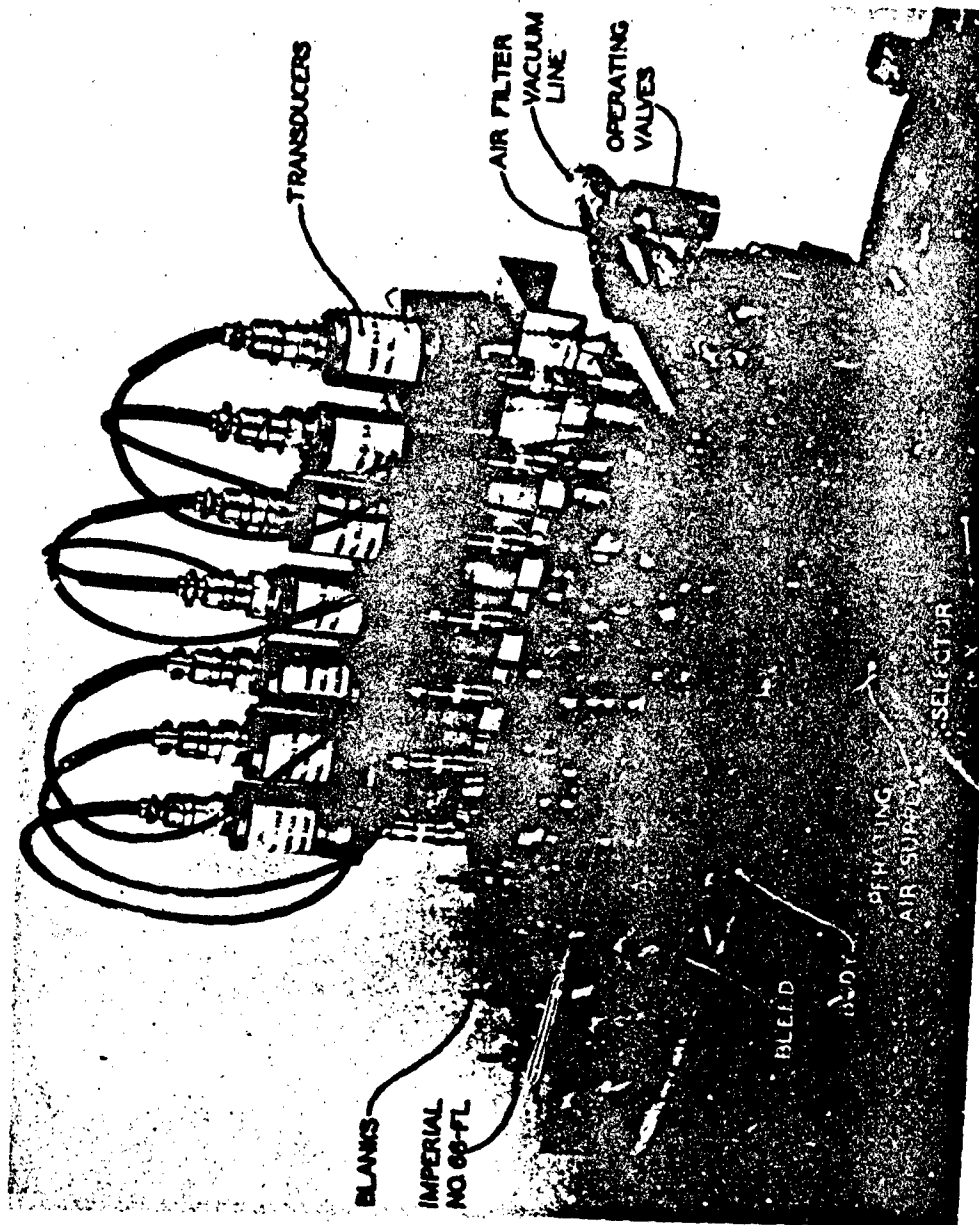
Figure 6. Pressure Scanner System

Labels visible in figure: TRANSDUCERS, AIR FILTER, VACUUM LINE, OPERATING VALVES, BLANKS, IMPERIAL NO 66-FL, BLEED, BODY, OPERATING AIR SUPPLY, SELECTOR

----- THEORY OF REF. 5
——— METHOD OF CHARACTERISTICS

M = 3.50

M = 3.00

M = 2.50

P_2/P_∞

X/D

0 (CORNER)   .2   .4   .6   .8   1.0 (BASE)
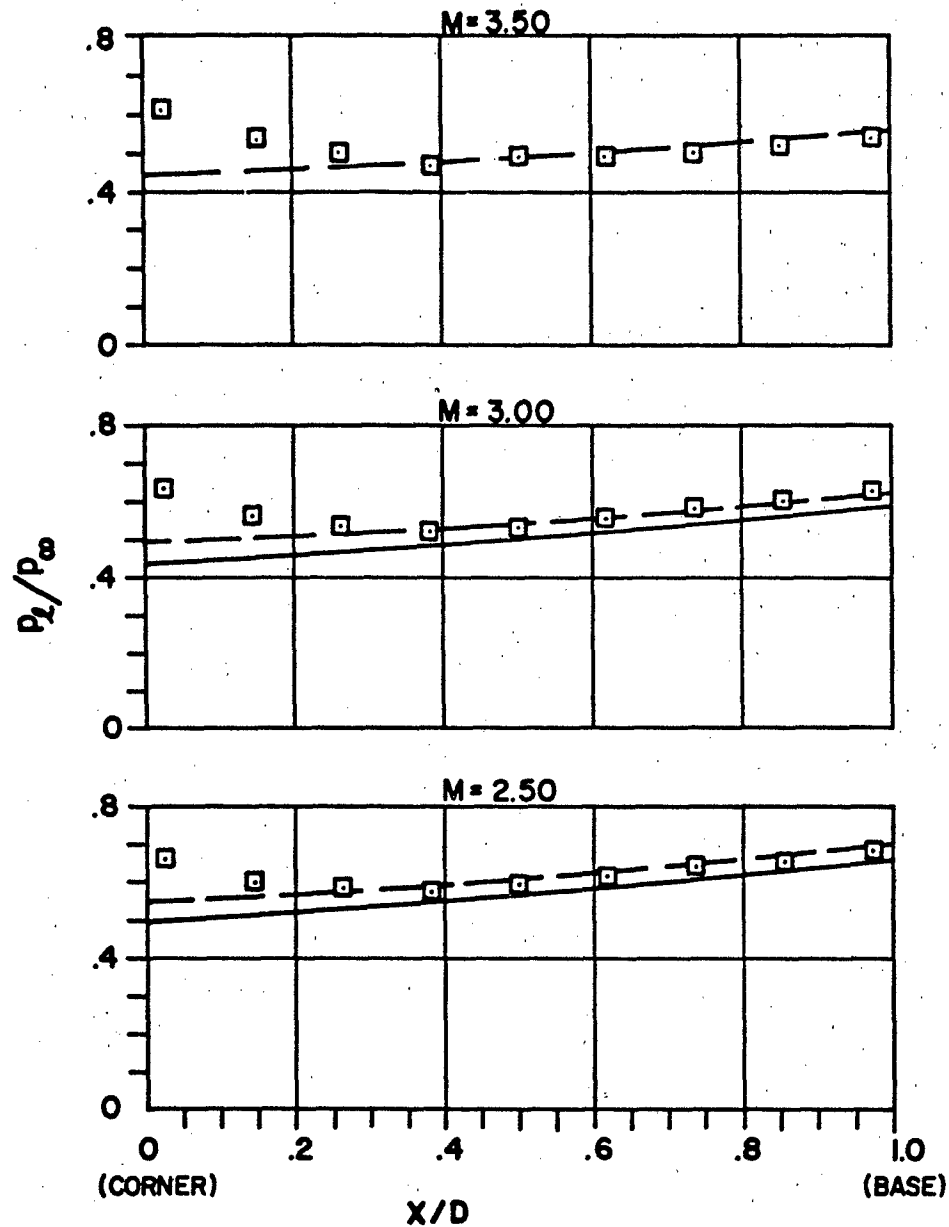
(a) Boattail No. 6

Figure 7. Boattail Pressure Distribution

26
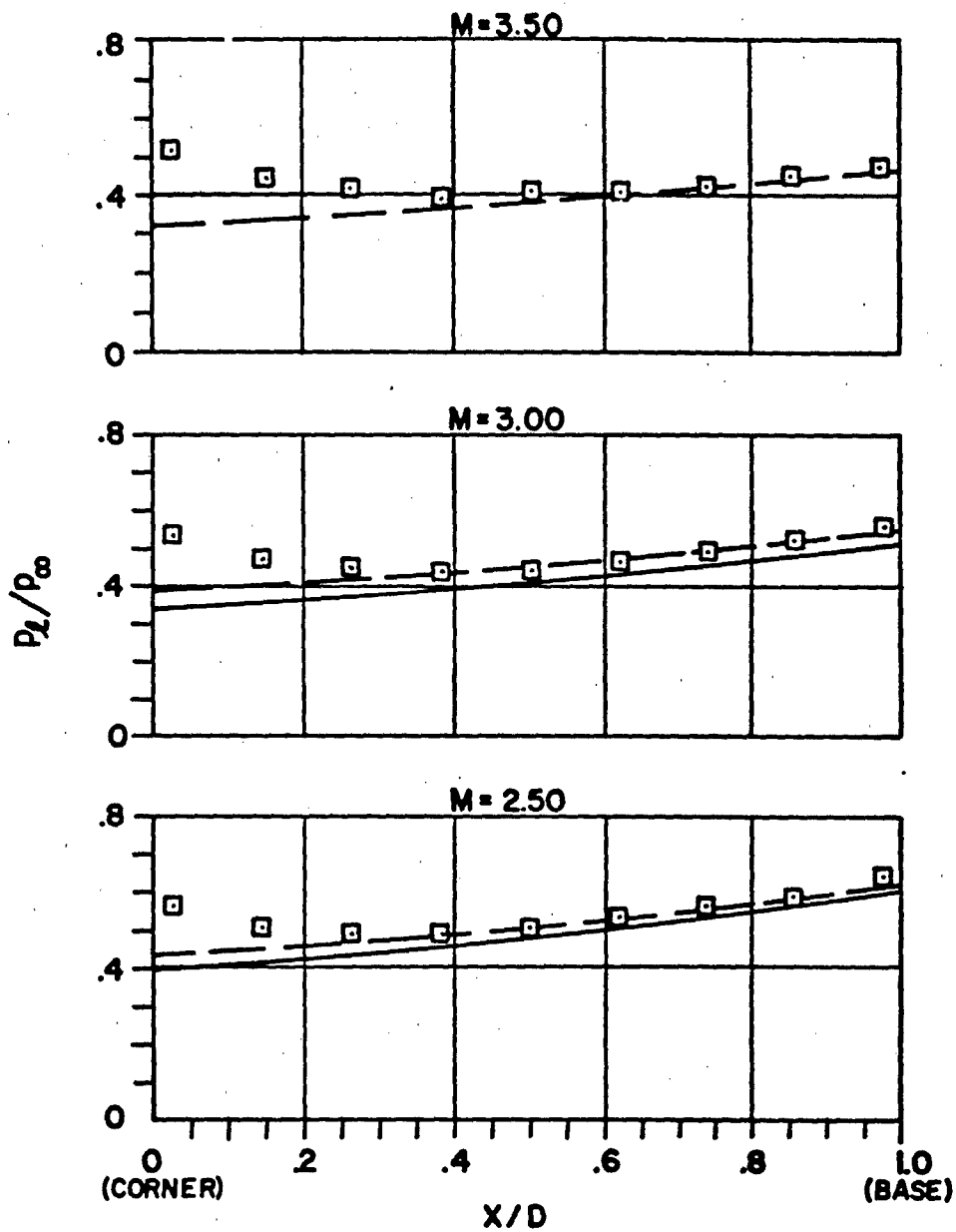
(b) Boattail No. 7

Figure 7. Continued

27
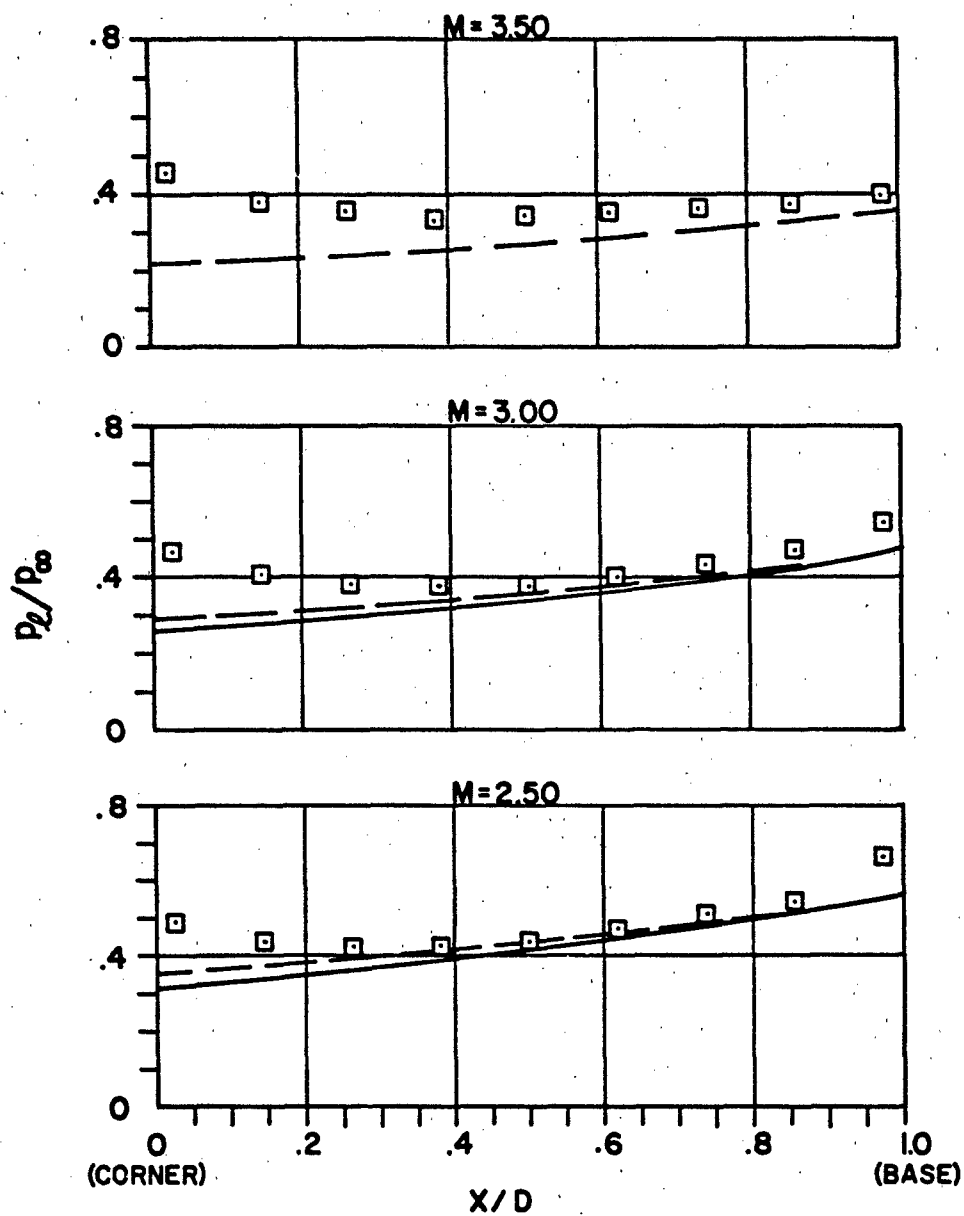
(c) Boattail No. 8

Figure 7. Continued
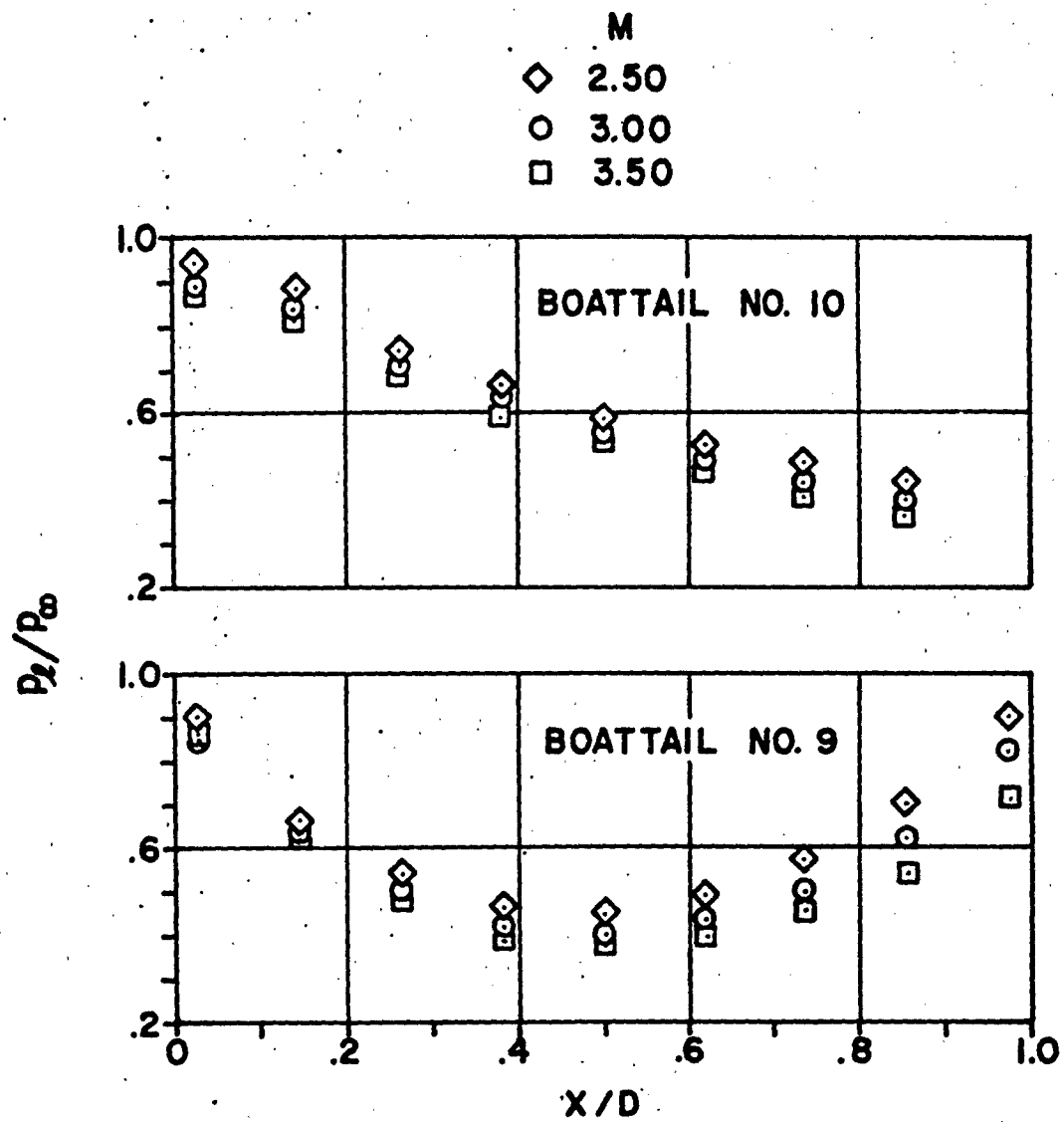
(d) Boattail Nos. 9 and 10

Figure 7. Continued

29

METHOD OF CHARACTERISTICS
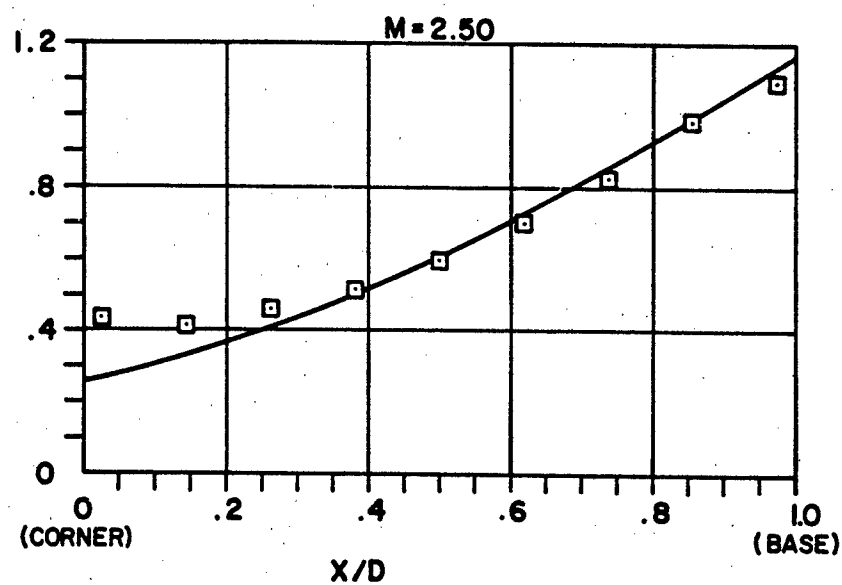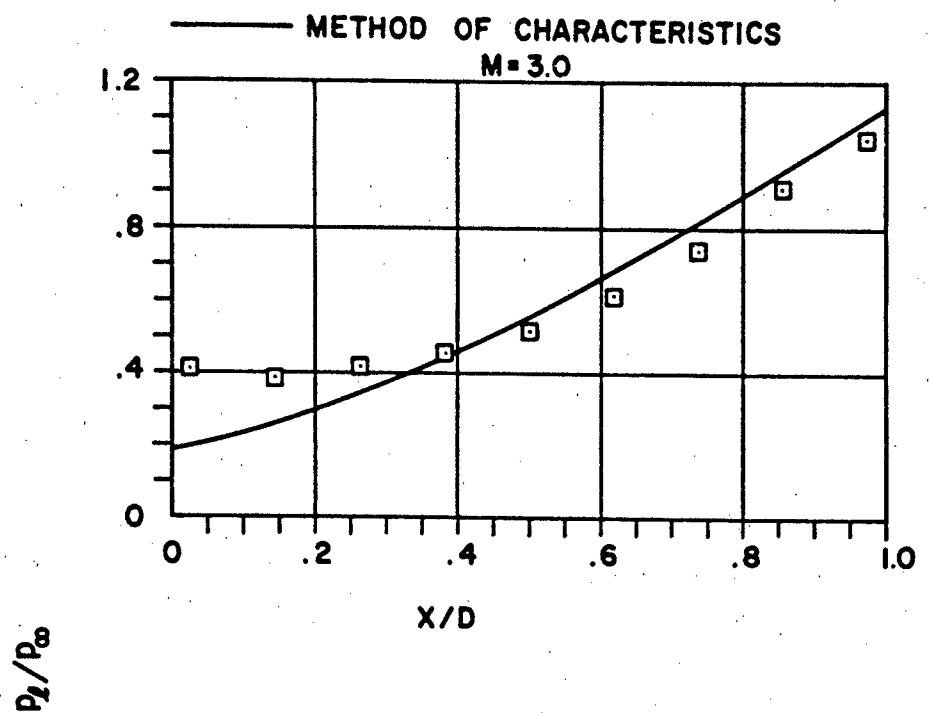
(e) Boattail No. 11

Figure 7. Concluded

30

Figure 8. Effect of Sustainer Nozzle Operating Pressure
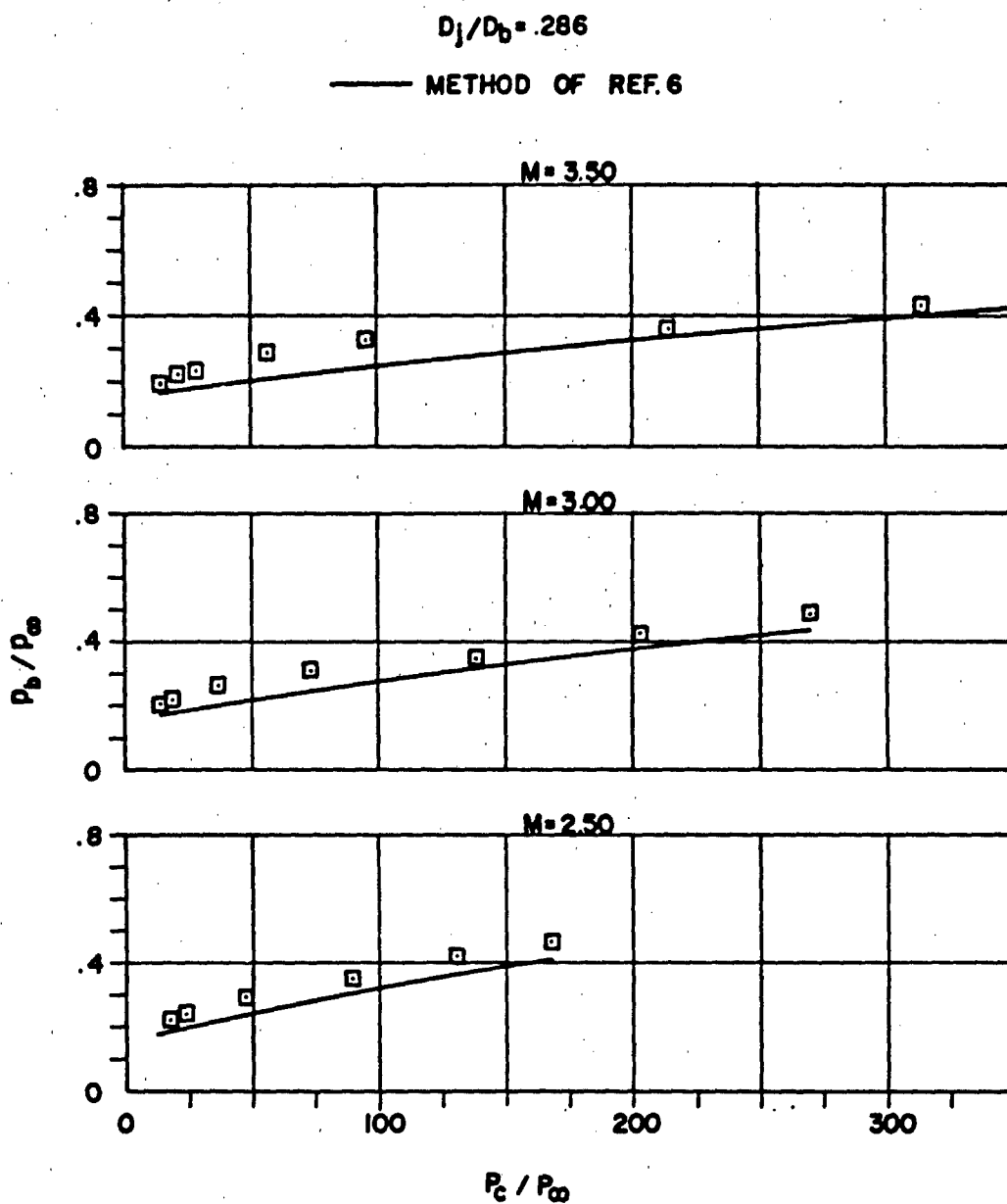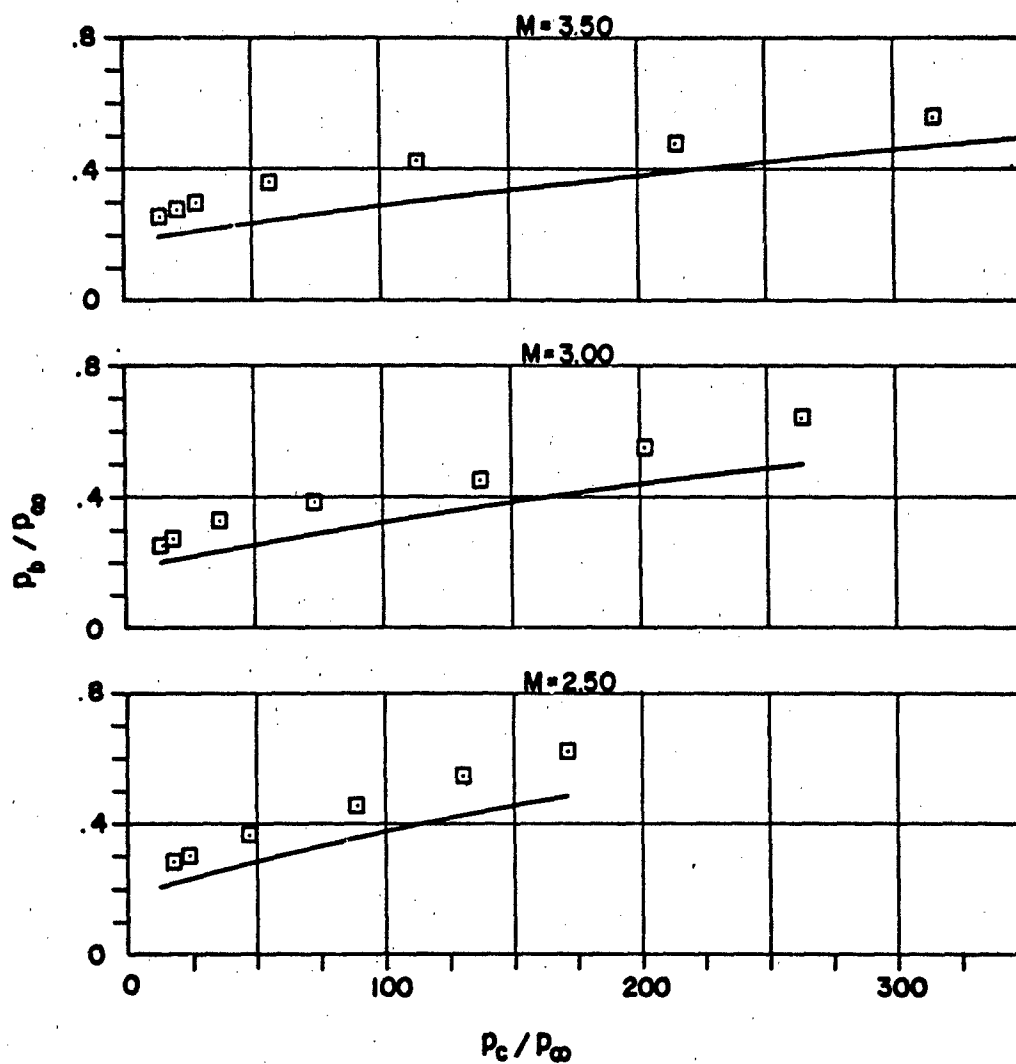on Boattail Drag
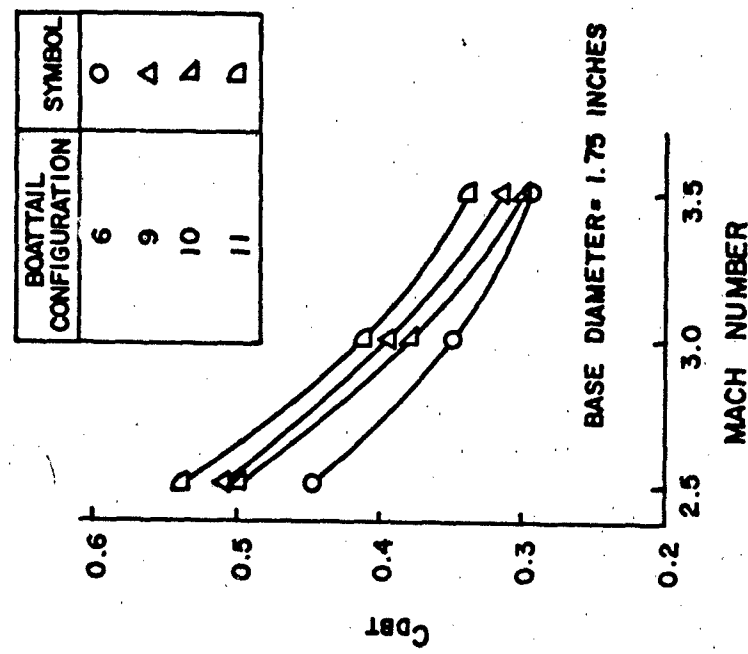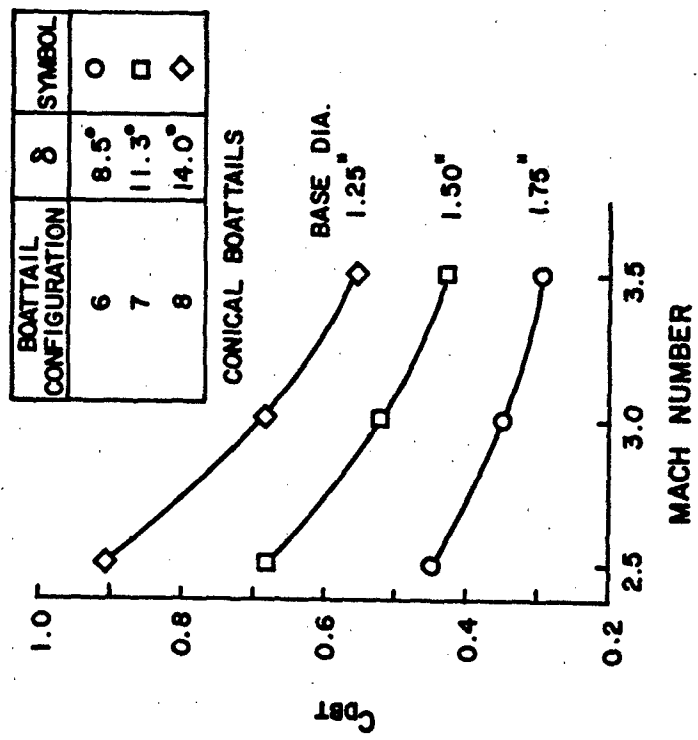
Figure 9. Effect of Mach Number on Boattail Drag

$D_j/D_b = .286$

——— METHOD OF REF.6

(a) Configuration No. 6

Figure 10. Effect of Sustainer Nozzle Operating Pressure on Base Pressure
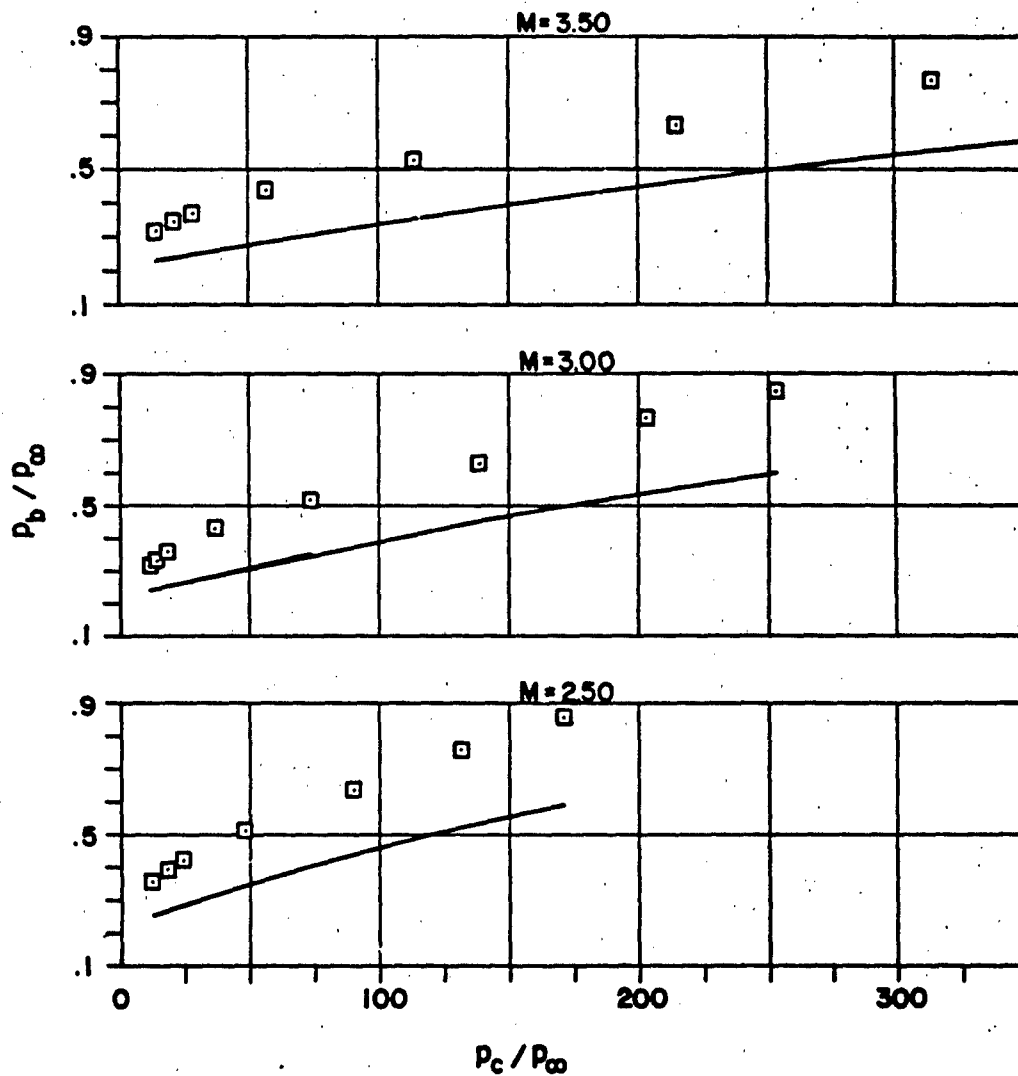
33

$D_j/D_b = .333$

——— METHOD OF REF. 6

M = 3.50

M = 3.00

M = 2.50

p_b / p_∞

p_c / p_∞

(b) Configuration No. 7

Figure 10. Continued

$D_j/D_b = .400$

——— METHOD OF REF. 6

(c) Configuration No. 8

Figure 10. Concluded

$D_j / D_b = .286$

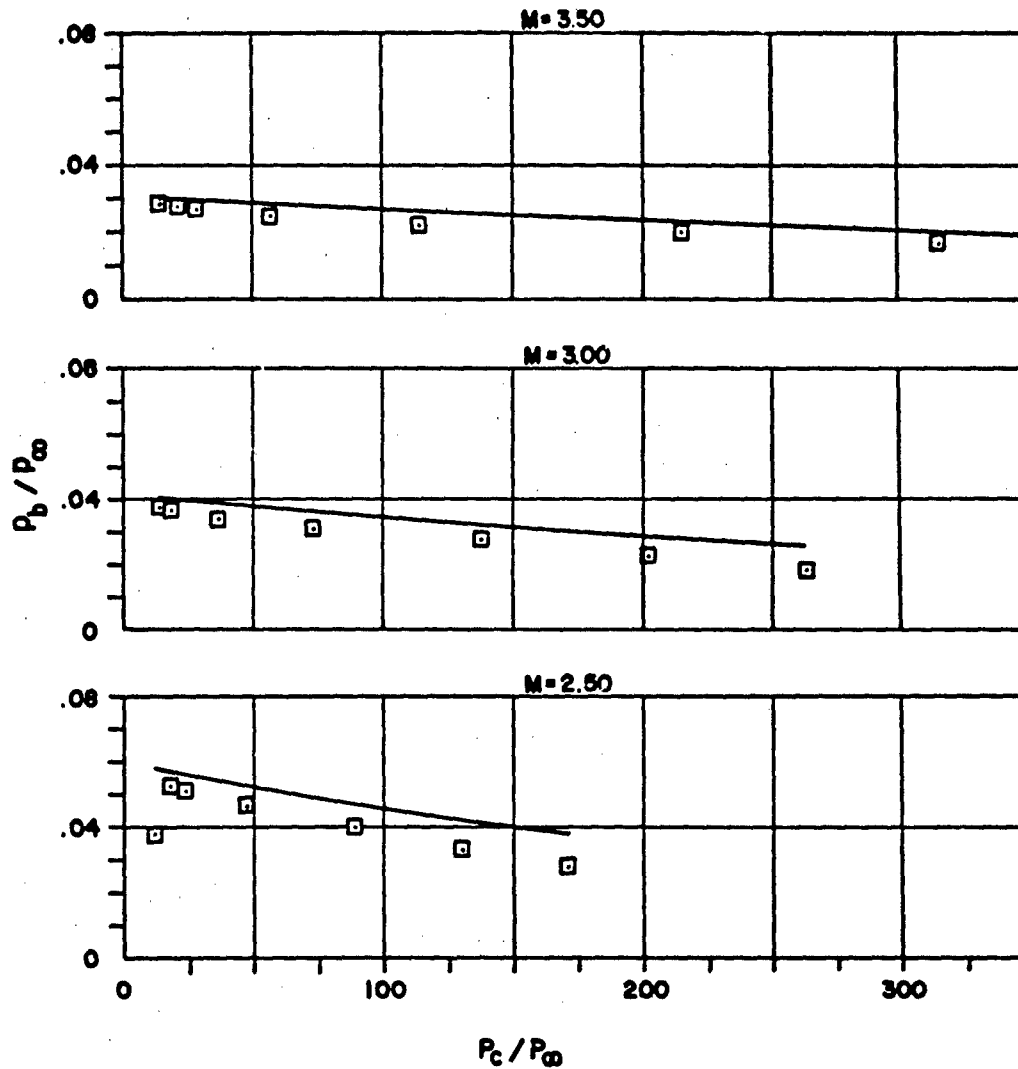—— METHOD OF REF. 6

M = 3.50

M = 3.00

M = 2.50

P_c / P_∞
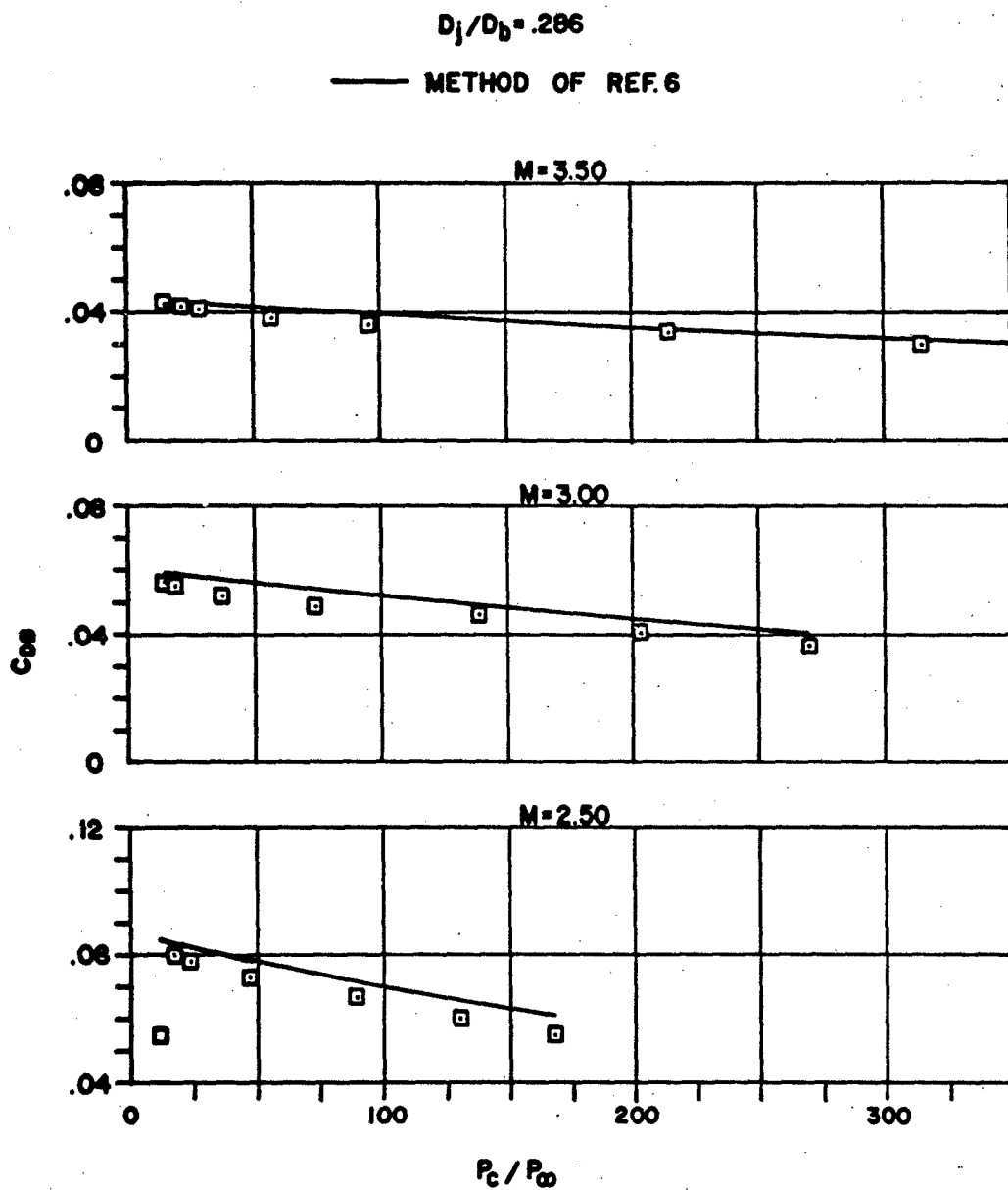
(a) Configuration No. 6

Figure 11. Effect of Sustainer Nozzle Operating Pressure
on Base Drag

36

$D_j/D_b = .333$

—— METHOD OF REF. 6

M = 3.50

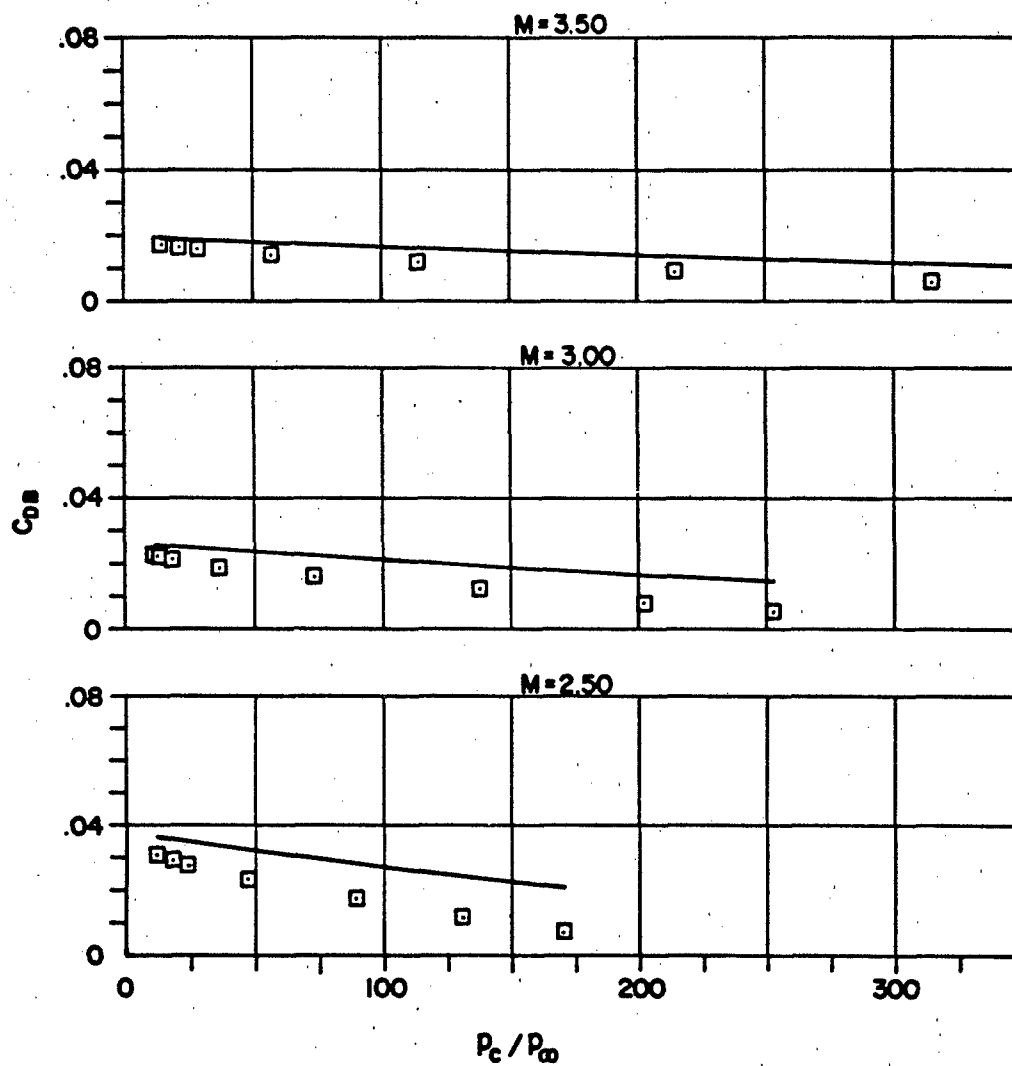M = 3.00

M = 2.50

P_c/P_∞

(b)   Configuration No. 7

Figure 11.   Continued

37

$D_j/D_b = .400$

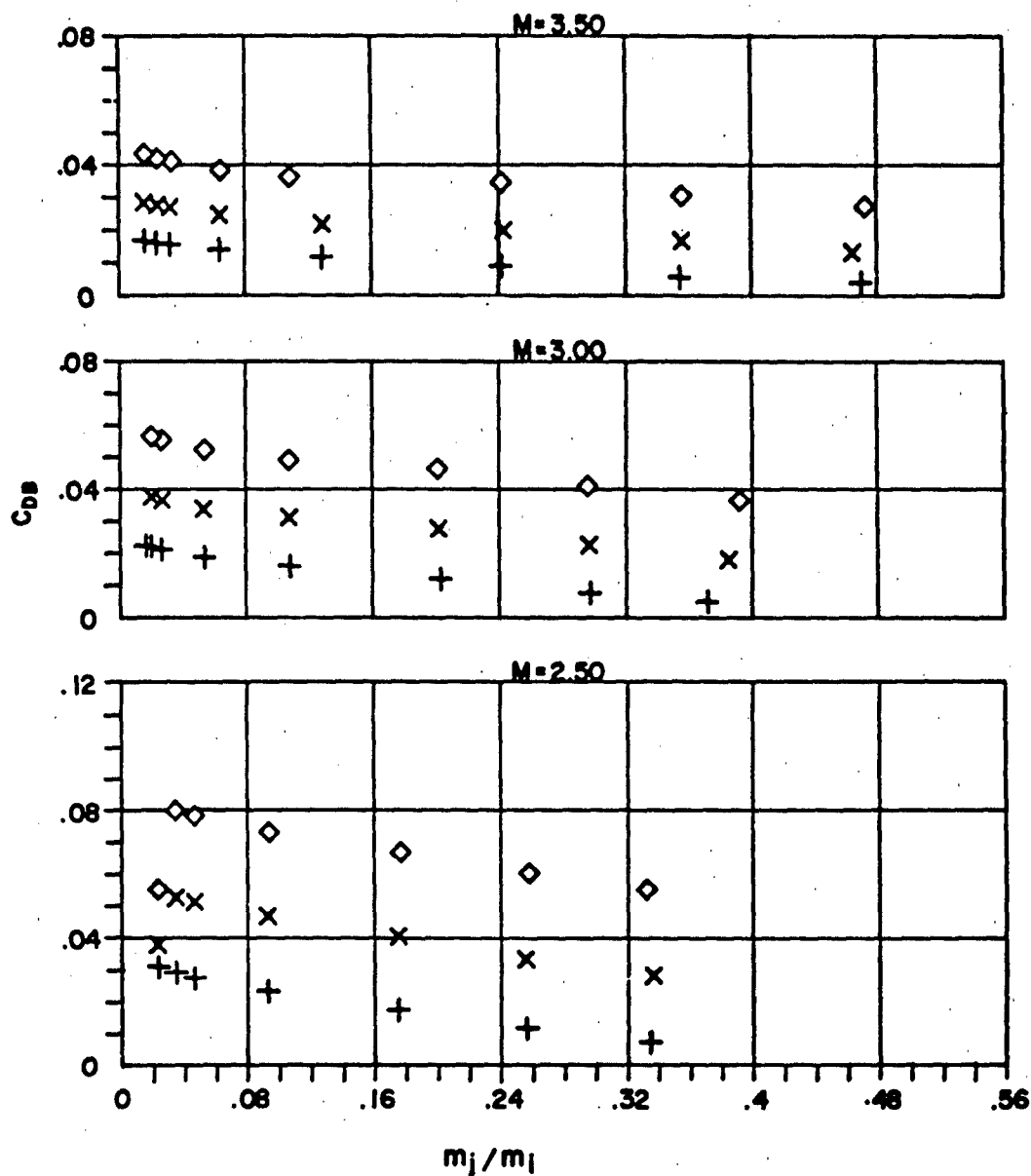——— METHOD OF REF. 6

(c) Configuration No. 8

Figure 11. Concluded

◇ CONFIGURATION   NO. 6 (D_j/D_b=.286)
✕ CONFIGURATION   NO. 7 (D_j/D_b=.333)
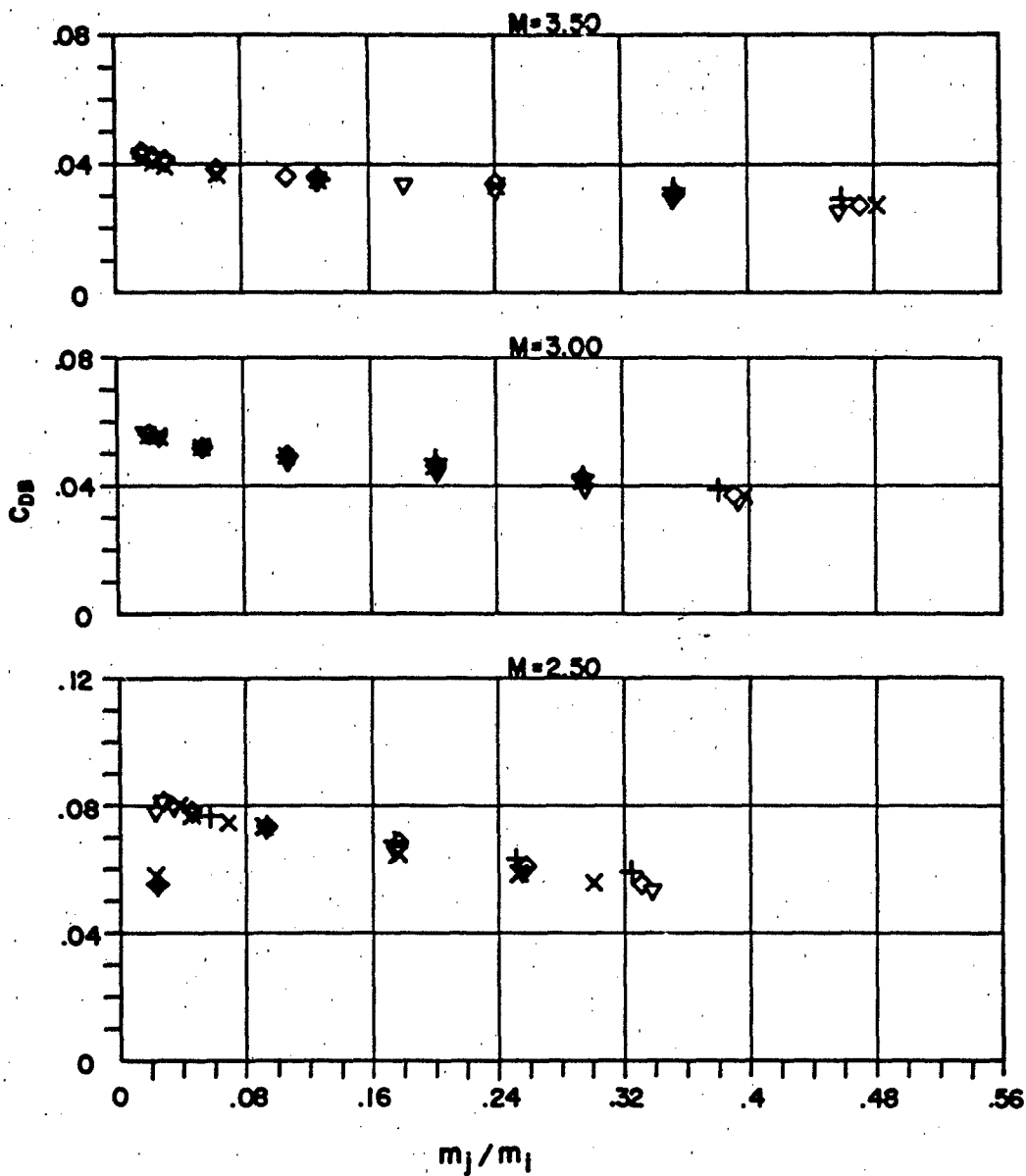+ CONFIGURATION   NO. 8 (D_j/D_b=.400)

(a)   Configuration Nos. 6, 7 and 8

Figure 12.   Effect of Jet Mass Flow on Base Drag

◇ CONFIGURATION NO. 6
✕ CONFIGURATION NO. 9
+ CONFIGURATION NO. 10
▽ CONFIGURATION NO. 11

$D_j/D_b = .286$

M=3.50

M=3.00

M=2.50

C_{DB}

m_j/m_i

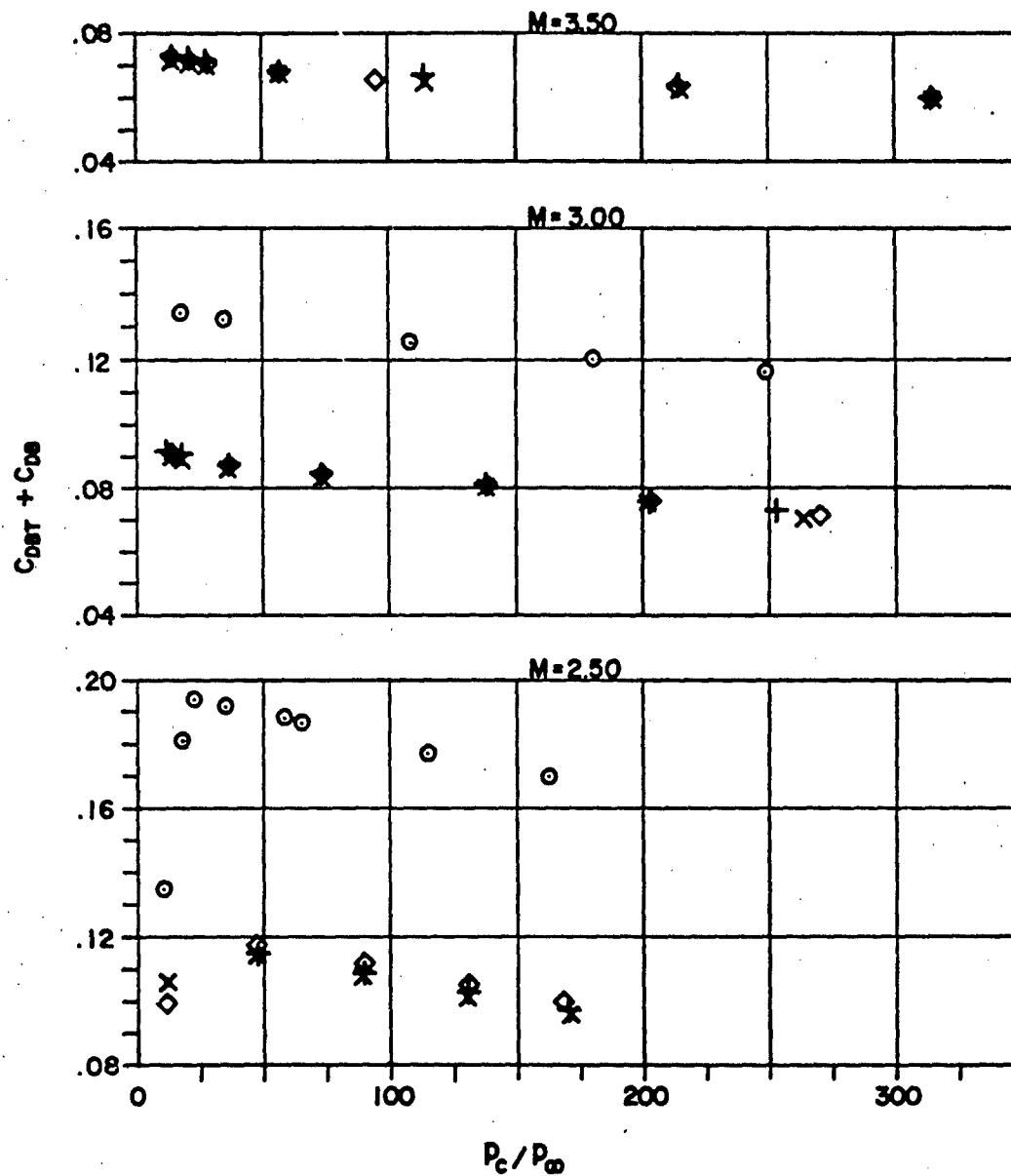(b) Configuration Nos. 6, 9, 10 and 11
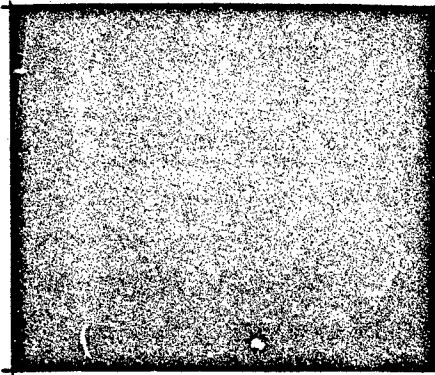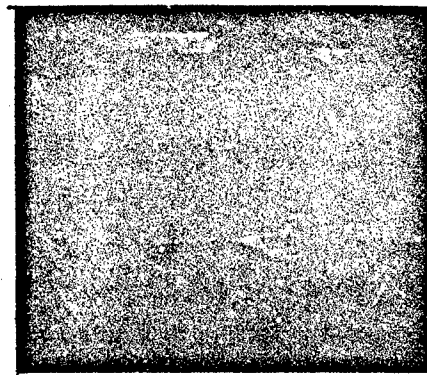
Figure 12. Concluded

40

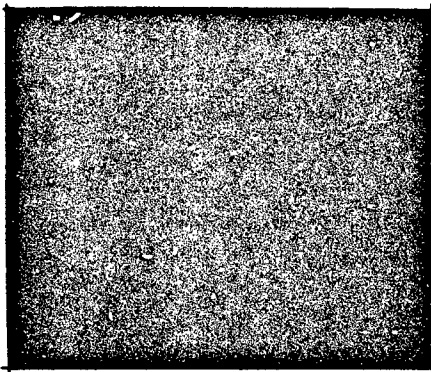Figure 13. Effect of Sustainer Nozzle Operating Pressure
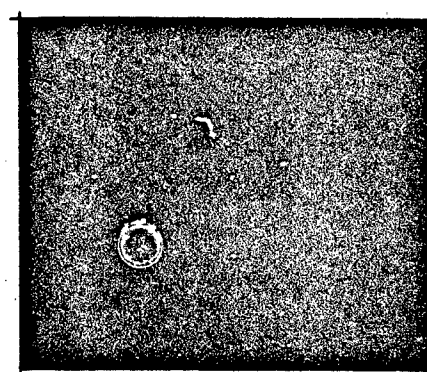on Total Drag

41

$P_c / P_\infty = 0$

$P_c / P_\infty = 168$

M = 2.50

$P_c / P_\infty = 0$

$P_c / P_\infty = 315$

M = 3.50

Figure 14.   Schlieren Photographs of Base Flow Field
for Boattail No. 6

REFERENCES

1. J. C. McMullen, "Wind Tunnel Testing Facilities at the Ballistic Research Laboratories," BRL Memorandum Report No. 1292, July 1960.

2. C. C. Bush, "Flow Characteristics of the Ballistic Research Laboratories' Supersonic Wind Tunnel No. 1," BRL Memorandum Report No. 1731, February 1966.

3. R. Colburn, "Pressure Scanner Unit," BRL Technical Note No. 1616, June 1966.

4. Ames Research Staff, "Equations, Tables and Charts for Compressible Flow," NACA Report No. 1135, 1953.

5. C. A. Syvertson and D. H. Dennis, "A Second-Order Shock-Expansion Method Applicable to Bodies of Revolution Near Zero Lift," NACA Report No. 1328, 1957.

6. C. E. Brazzel and J. H. Henderson, "A Correlation of the Base Drag of Bodies of Revolution With a Jet Exhausting Through the Base," Paper presented at Army Science Conference, 1966.

7. J. Huerta, "The Effect of Rocket Nozzle Geometry and Secondary Flow Field on Base Drag at Mach Numbers 2.50 and 3.00, An Experimental Investigation," BRL Memorandum Report No. 1829, March 1967.

DOCUMENT CONTROL DATA - R & D

(Security classification of title, body of abstract and indexing annotation must be entered when the overall report is classified)

1. ORIGINATING ACTIVITY (Corporate author)	2a. REPORT SECURITY CLASSIFICATION
U.S. Army Aberdeen Research and Development Center Ballistic Research Laboratories Aberdeen Proving Ground, Maryland	Unclassified
	2b. GROUP

3. REPORT TITLE

AN EXPERIMENTAL INVESTIGATION AT SUPERSONIC MACH NUMBERS OF BASE DRAG OF VARIOUS BOATTAIL SHAPES WITH SIMULATED BASE ROCKET EXHAUST

4. DESCRIPTIVE NOTES (Type of report and inclusive dates)

5. AUTHOR(S) (First name, middle initial, last name)

Joseph Huerta

6. REPORT DATE	7a. TOTAL NO. OF PAGES	7b. NO. OF REFS
June 1969	46	7

8a. CONTRACT OR GRANT NO.	9a. ORIGINATOR'S REPORT NUMBER(S)
b. PROJECT NO. RDT&E Project No. 1T061102A33D	Memorandum Report No. 1983
c.	9b. OTHER REPORT NO(S) (Any other numbers that may be assigned this report)
d.	

10. DISTRIBUTION STATEMENT

This document is subject to special export controls and each transmittal to foreign governments or foreign nationals may be made only with prior approval of Commanding Officer, U.S. Army Aberdeen Research and Development Center, Aberdeen Proving Ground, Maryland.

11. SUPPLEMENTARY NOTES	12. SPONSORING MILITARY ACTIVITY
	U.S. Army Materiel Command Washington, D.C.

13. ABSTRACT

An experimental investigation was conducted to determine the effect of boattail geometry and simulated base rocket nozzle flow on overall base drag. All tests were performed at Mach numbers 2.50, 3.00 and 3.50. Reasonable prediction of base drag for the reported boattail shapes can be made by using approximate and empirical equations. A conical boattail produced less drag than the other boattail shapes investigated. The maximum nozzle stagnation to free-stream pressure ratio reported is 315.

DD FORM 1473 REPLACES DD FORM 1473, 1 JAN 64, WHICH IS OBSOLETE FOR ARMY USE.

14. KEY WORDS	LINK A		LINK B		LINK C	
	ROLE	WT	ROLE	WT	ROLE	WT
Supersonic Flow						
Base Drag						
Base Rocket						
Boattail Drag						
Base Pressure						
Boattail Pressure						